

# CEBAF Beam Viewer Imaging Software\*

B. A. Bowling, C. McDowell

Continuous Electron Beam Accelerator Facility  
12000 Jefferson Avenue, Newport News, VA 23606-1909 USA

## Abstract

This paper discusses the various software used in the analysis of beam viewer images at CEBAF. This software, developed at CEBAF, includes a three-dimensional viewscreen calibration code which takes into account such factors as multiple camera/viewscreen rotations and perspective imaging, and maintaining a calibration database for each unit. Additional software allows single-button beam spot detection, with determination of beam location, width, and quality, in less than three seconds. Software has also been implemented to assist in the determination of proper chopper RF control parameters from digitized chopper circles, providing excellent results.

## I. INTRODUCTION

CEBAF uses phosphorous beam viewer devices for initial beam setup and for visual observations of beam spot quality. The viewscreens, made of a chromium-doped alumina material, are inserted into the beamline using pneumatic plunger devices, with the resultant image being captured via a Sony vidicon CCTV camera, and displayed in the control room using closed-circuit monitors (fig. 1). The video signal is also fed into a 512x512 8-bit video frame grabber, which is operationally controlled from software.

Some viewscreens at CEBAF are oriented on the beamline in the familiar 45 degree angle relative to the beam axis, with the camera mounted 90 degrees facing the viewscreen. The majority of the viewscreens, however, in addition to the above geometry, are mounted at a 45 degree angle axially rotated relative to the beamline, and the camera is similarly rotated 45 degrees relative to the camera axis. The complex 3-dimensional rotations encountered by the digitized image due to these physical mountings, as well as pronounced depth-perception effects caused by the relatively close proximity of the cameras, ruled out the use of any of the available off-the-shelf imaging software known by the authors. It was therefore required to develop the calibration software in-house, which was customized for use with the viewscreens in use at CEBAF. This software allows for individual viewscreen positional calibration, with the results entered into a database for use by other application programs.

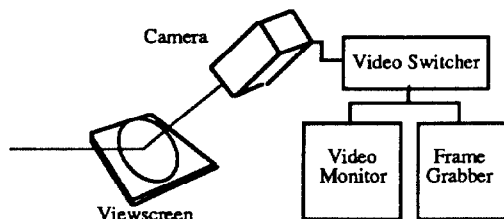


Figure 1. Camera System Diagram

\* Supported by U. S. DOE contract DE-Ac05-84ER40150

Other imaging software developed and currently in use at CEBAF includes an automated beam spot detector, which when activated performs a digitization of the currently inserted viewscreen and determines spot centroid position, spot width, and spot quality. Another specialized code performs analysis of an image of the chopping ellipse, providing steering, amplitude and phase information directly applicable to the chopper controls.

## II. CALIBRATION SOFTWARE

Each viewscreen used at CEBAF consists of a phosphorous plate contained in a stainless-steel retaining fixture, which exposes a circular area of phosphorous 1.125 inch in diameter. Each viewscreen is precisely CNC machined, and the pneumatic plunger device provides extremely accurate and reproducible placement of the screen within the beampipe. Similarly, the camera mounting on the beamline is very rigid, generating negligible movements in the cameras. This quality setup allows the frame of the viewscreen to be the calibration fiducial, greatly simplifying the calibration software.

An outline of the viewscreen frame was created within the calibration software. The calibration code provides an outline which is overlaid on the currently digitized viewscreen image. The outline can be translated, rotated, and/or adjusted for perspective imaging by the attached knob board. The rotation matrices used consists of rotations in the order of x, y, and z, and can be combined to yield:

$$R(\theta_x, \theta_y, \theta_z) = \begin{bmatrix} \cos \theta_y \cos \theta_z & -\cos \theta_y \sin \theta_z & \sin \theta_y & 0 \\ \cos \theta_x \sin \theta_z \sin \theta_y + \cos \theta_x \cos \theta_z & -\sin \theta_x \sin \theta_z \sin \theta_y & -\sin \theta_x \cos \theta_z & 0 \\ -\sin \theta_y \cos \theta_z \cos \theta_x + \sin \theta_y \sin \theta_z & \sin \theta_y \sin \theta_z \cos \theta_x + \cos \theta_y \sin \theta_z & \cos \theta_y \cos \theta_z & 0 \\ 0 & 0 & 0 & 1 \end{bmatrix}$$

Translation is handled by the following matrix:

$$T(T_x, T_y, T_z) = \begin{bmatrix} 1 & 0 & 0 & 0 \\ 0 & 1 & 0 & 0 \\ 0 & 0 & 1 & 0 \\ T_x & T_y & T_z & 1 \end{bmatrix}$$

The cameras are mounted relatively close to the beamline, accentuating perspective imaging effects<sup>1,2</sup>. This is taken into account by the following perspective matrix:

$$P(x, y, z) = \begin{bmatrix} 1 & 0 & 0 & 0 \\ 0 & 1 & 0 & 0 \\ 0 & 0 & 0 & \frac{1}{f} \\ 0 & 0 & 1 & 0 \end{bmatrix}$$

The user acquires the image, which is automatically displayed on the computer screen as a gray-scale image and adjusts the rotation angle, translation, and perspective values until the viewscreen outline overlies the image properly. When the user is satisfied with the calibration, the save button is

activated, saving the angles, translations, and perspective values. These calibration values are maintained in a database file for each viewscreen, available for use by all imaging codes.

The camera calibration program also allows one to use the mouse arrow to point to a particular area on the viewplate image, displaying the equivalent beam coordinate in millimeters, using the pre-determined calibrations. An automated beam spot detection algorithm is also available in this code which determines spot location, width, and quality, which is described in the next section.

### III. INSTAMATIC BEAM DETECTOR

To aid in the analysis of digitized beam spots, the INSTAMATIC automatic beam detection and analysis software was developed at CEBAF<sup>3</sup>. The design goal of this code was to quickly determine beam location on the currently-inserted viewscreen to aid in rough beam tune-up and beam analysis. With a single click of a button, the frame grabber captures the image and INSTAMATIC performs the spot analysis in less than three seconds, achieving the design goals

The spot detection algorithm starts by determining an intensity threshold in which the beam spot pixel must exceed in order to be considered. The digitized images exhibit speckle and slow intensity variations, which required a somewhat robust threshold determination. The threshold is determined from pixel values located around the outer perimeter of the viewplate, where the beam can never be present:

$$\langle I \rangle = \frac{\sum_{k=1}^n I_k}{n}$$

$$I_o = \langle I \rangle + 2 \left[ \frac{1}{n-1} \left\{ \sum_{k=1}^n I_k^2 - \frac{\left( \sum_{k=1}^n I_k \right)^2}{n} \right\} \right]^{\frac{1}{2}}$$

The algorithm now determines the approximate location of the beam spot within the digitized grid array. One cannot simply seek out the brightest digitized grid value, due to the aforementioned speckle. The method implemented uses two pieces of information to determine the location of the spot; one looks at the intensity of a given pixel, choosing the pixel with the greatest intensity, and the other averages the eight neighboring pixels surrounding the given pixel, choosing favorably neighbors with little deviation. The two are combined to yield

$$G(i,j) = \frac{I(i,j)}{256} * \left( 1 - \frac{\sum_{k=1}^{i+1} \sum_{l=j-1}^{j+1} (I(i,j)I(k,l)) * (1 - \delta_{(ik)}\delta_{(jl)})}{8(I(i,j) + 1)} \right)$$

This equation is performed for each pixel contained on the phosphorous area of the plate, and the value of  $G$  which is greatest is chosen as the spot location. This detection equation

performs very well, operates fast, and was simple to implement.

The above equation locates the spot in a general region. However, due to spot variations like speckle, this usually is not the centroid of the beam. The centroid pixel location is determined by a center-of-mass calculation which recursively spawns itself off within the spot, similar to a flood-fill graphics algorithm. Additionally, a center-of-area computation is performed determining the pixel which best lies in the center of the spot outline. The distance from the center-of-mass pixel to the center-of-area is defined as the quality factor; with perfect spots these two criteria are at the same pixel.

### IV. GINSU CHOPPER CIRCLE ANALYZER

CEBAF utilizes a chopping system which consists of two identical RF cavities producing a transverse rotary motion in the beam. The beam is passed through a 60 degree aperture plate, to achieve the chopping. The aperture is removable and can be replaced by a viewscreen to allow a visual inspection of the rotary beam motion.

The size and centering of the chopping ellipse are very critical. In the past, mechanical means were used for determining proper elliptical parameters, such as the use of calipers on the image produced on the CCTV monitor. A more automated method was required for this setup, giving birth to the GINSU chopper alignment code<sup>4</sup>, developed at CEBAF. This program uses the frame grabber to snapshot a picture of the chopping circle and performs a least-squares fit to parametric equations defining the ellipse, determining the amplitude and relative phase slip in the digitized image. This information can be fed directly into the RF controls, performing a feedback in order to improve the ellipse.

When the image of the ellipse is acquired, the GINSU code starts its analysis by detecting the ellipse within the digitized data. This is accomplished by sending out rays at constant angular increments from the calibrated center of the viewscreen, comparing each pixel value and saving the location (pixel row and column) containing the brightest pixel. This produces a pair of  $x,y$  locations as a function of angle from the ray, tracing out a circle from 0 to 360 degrees, as in figure 2.

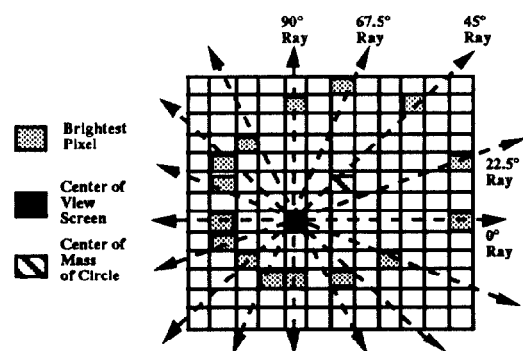


Figure 2. GINSU Ray Operation.

The rays are sent out with the calibration center being the point of origin. However, the ellipse may not be properly centered on the viewscreen, which will result in vastly unequal distances between data points (see fig. 2). From this, however, it is possible to determine the true center from a center-of-mass calculation, taking the irregular point spacings:

$$\langle X \rangle = \frac{\sum_{i=1}^n X_i \rho_i}{\sum_{i=1}^n \rho_i}; \quad \langle Y \rangle = \frac{\sum_{i=1}^n Y_i \rho_i}{\sum_{i=1}^n \rho_i}; \quad \rho_i = \sqrt{(X_i - X_{(i-1)})^2 + (Y_i - Y_{(i-1)})^2}$$

Once this location has been determined, the rays are sent out again using this new location as the center, and these final pixel row and column locations are used.

The chopping ellipse is generated by an RF cavity which is driven in both the horizontal and vertical planes, and which is described parametrically as:

$$X = A \cos(2\pi\omega t) \\ Y = B \sin(2\pi\omega t + \phi)$$

A least-squares fit can be performed on the digitized image using the following minimization criterion:

$$S = \sum_{\theta=0}^{2\pi} (B \sin(\theta + \phi) - Y(\theta))^2$$

This expression cannot be directly minimized due to the phase parameter within the transcendental function. However, a solution can be obtained by computing  $S$  for various values of  $\phi$  and using the phase value which yield the best minimum, with  $B$  defined as:

$$B = \frac{\sum_{\theta=0}^{2\pi} Y(\theta) \sin(\theta + \phi)}{\sum_{\theta=0}^{2\pi} \sin^2(\theta + \phi)}$$

The computed values of  $B$  and  $\phi$  can be directly applied to the RF control system to improve the ellipse. The determined centroid values provide relevant information about steering correction. The fitted amplitudes are within 20 percent, and the computed phase angle is usually within plus or minus 5 degrees. This accuracy generally results in one application of correction to the RF system to obtain a proper chopper ellipse.

During chopper setup using the viewscreen, it was noticed that the elliptical image would slowly drift and radially expand, which was due to charge deposition on the view plate from the beam. This results in erroneous steering computations, as well as distortions in the ellipse image with corresponding errors in the GINSU phase and amplitude results. This problem was alleviated by triggering the frame grabber off of the beam sync, which is generated by the gun interface module. The accelerator is operated in the single-shot mode, which provides the minimum amount of time

required to digitize the image, practically eliminating the charge deposition problem.

## V. REFERENCES

- [1] P. K. Kloeppe, B. A. Bowling, and M. E. Wise, "Linearity Tests on the CEBAF Viewer System", CEBAF-TN-026(1991).
- [2] S. Jin, P. K. Kloeppe, "Error Analysis of the Beam Viewer System for Quantitative Measurements", CEBAF-TN-91-088(1991).
- [3] B. Bowling, C. McDowell, "Automatic Beam Spot Detection for the CEBAF Camera System", CEBAF-TN-012 (1992).
- [4] B. Bowling, P. K. Kloeppe, and G. Krafft, "Determining Chopper Alignment with the CEBAF Camera System", CEBAF-TN-91-108(1991).